Department of Pesticide Regulation

Brian R. Leahy
Director

M E M O R A N D U M

Edmund G. Brown Jr.
Governor

TO: Pam Wofford
Environmental Program Manager I
Environmental Monitoring Branch

Original signed by

FROM: Frank Spurlock, Ph.D.
Research Scientist III

DATE: July 20, 2015

SUBJECT: VARIABILITY IN SIMULATED CHLOROPICRIN AND 1,3-DICHLOROPROPENE VOLATILIZATION FROM BARE GROUND BROADCAST APPLICATIONS.

SUMMARY

Bulk density, soil water content and saturated water content data from 121 soil cores collected in 15 fields prior to pre-plant fumigation were used in HYDRUS simulations of chloropicrin (PIC) and 1,3-dichloropropene (13D) flux. Cumulative flux (emission ratio, ER = cumulative flux/applied fumigant) and discrete maximum 6 h period-mean flux density (max flux, ug m^{-2} s^{-1}) were simulated for shallow (12 inch) and deep (18 inch) bare ground broadcast applications using the compiled soil data. The objective of the modeling was to estimate mean, within-field variability, and between-field variability of ER and max flux. Quantifying the modeled variability will set a lower bound on the variability one could expect in commercial applications. The results provide (a) a statistical context for understanding HYDRUS-modeled fluxes, (b) a frame of reference for evaluating field-based flux data from individual studies, and (c) allow development of stochastic flux estimates for use in exposure assessment. This memo describes the modeling procedure and results. Primary conclusions of this modeling study are:

- The grand mean of modeled ER and max flux over 15 fifteen fields agreed favorably with existing field-based estimates of shallow and deep bare ground broadcast applications. This supports the veracity of the modeling procedures,
- Coefficients of variation (CV) for field-mean max flux were greater than for field-mean ER, and both increased with increasing depth of application.
- Between-field variability for both ER and max flux is generally greater than within-field variability based on a comparison of the respective CVs.
- Field-mean max flux for each fumigant-depth of application scenario were adequately described by a Normal distribution based on a non-significant Anderson-Darling statistic (A-D, $\alpha = 0.05$). However, fits to several other distributions also yielded non-significant A-D statistics. If a goal is to generate max flux distributions for Monte Carlo analysis, a distributional goodness of fit analysis should first be conducted to determine the best fit distribution for sampling.

INTRODUCTION

Soil preparation prior to pre-plant soil fumigations typically entails tillage operations such as chiseling, ripping and disking, followed by irrigation to bring the soil to fumigant label-required water contents. Gravimetric water content (*GWC*, g water/g soil) and soil bulk density (*BD*, g cm^{-3}) were measured in a total of 113 soil cores sampled from 12 fields in the recent soil variability study (study 285, Johnson and Tuli, 2013) and 3 fields in the Lost Hills study (Spurlock et al., 2013b). The cores were collected after tillage and irrigation operations were completed, and within 24 hours prior to fumigation. These measured properties were used to calculate saturated water content, (*Sat WC*, cm^3 water (cm^{-3} bulk soil), assumed equal to total porosity:

$$Sat\ WC = 1 - (\frac{\mathrm{BD}}{2.65})$$

where 2.65 g cm^{-3} is the assumed soil particle density for mineral soils (Freeze and Cherry, 1979). In addition, volumetric water content (*WC*, cm^3 water (cm^{-3} bulk soil) was calculated:

$$WC = BD\ x\ GWC$$

WC and *Sat WC* are the soil variables for which HYDRUS 2D/3D modeled fumigant fluxes are most sensitive (Spurlock, 2013a). *BD* is also a HYDRUS input, but with a lesser direct effect on simulated fluxes. One goal of the soil variability study (Johnson and Tuli. 2013) was to provide data for estimating the resulting within and between-field variability in fumigant flux density and cumulative emissions.

BD, *WC* and *Sat WC* data from the 15 fields were used in HYDRUS flux modeling. Four to 12 cores were collected in each field, with the majority of fields having 8 or 9 cores sampled (Table 1). Soil properties were measured in the 0-10cm, 10-30 cm, and 30-50 cm soil core segments in the soil variability study. The three Lost Hills fields had the same soil data, but these were measured in the 0-20 cm, 20-40 cm, 40-60 cm and 60-80 cm depth core segments. HYDRUS simulations of chloropicrin (PIC) and 1,3-dichloropropene (13D) emission ratio (ER) and maximum 6 hr flux density (max flux, ug m^{-2} sec^{-1}, 100 lb applied per acre basis) were conducted for 12- and 18-inch deep (30 cm and 46 cm, respectively) untarped broadcast applications using the soil data for each core. ER is cumulative volatilization expressed as a fraction of fumigant applied; max flux is the maximum 6 h time averaged flux density among 6 h time periods as typically measured in field studies, e.g. 600 – 1200 h, 1200-1800 h, 1800 – 2400 h, etc. Mean soil organic carbon contents with depth from the 3 Lost Hills fields were assumed for all soils, and soil partition coefficients Kd were calculated using calibrated KOC values from Lost Hills study (Spurlock et al., 2013b). The remaining fumigant physicochemical properties are those used in previous HYDRUS modeling studies, including Lost Hills. Description of the modeling domains and other modeling details are given in Appendix 1. Within-field ER and max

flux means and within-field coefficients of variation (CV) were calculated for each field. The grand mean and between-field CV across all fields was calculated from the 15 field-mean ERs and max fluxes.

Table 1. Field information (N= number soil cores sampled in each field).

Location	Field name	N	Soil Texture	Core Segments
Crows Landing, Stanislaus Co.	cro1	8	CLAY LOAM	0-10, 10-30, 30-50cm
Dinuba, Tulare Co.	din1	8	SANDY CLAY LOAM	0-10, 10-30, 30-50cm
Dinuba, Tulare Co.	din2	8	SANDY LOAM	0-10, 10-30, 30-50cm
Lost Hills, Kern Co.	LH1	9	LOAM	0-20, 20-40, 40-60cm
Lost Hills, Kern Co.	LH2	4	LOAM	0-20, 20-40, 40-60cm
Lost Hills, Kern Co.	LH3	4	LOAM	0-20, 20-40, 40-60cm
Merced, Merced Co.	mer1	8	LOAM	0-10, 10-30, 30-50cm
Santa Maria, Santa Barbara Co.	san1	12	CLAY LOAM	0-10, 10-30, 30-50cm
Stockton, San Joaquin Co.	sto1	8	CLAY LOAM	0-10, 10-30, 30-50cm
Stockton, San Joaquin Co.	sto2	7	CLAY LOAM	0-10, 10-30, 30-50cm
Visalia, Tulare Co.	vis1	8	SANDY LOAM	0-10, 10-30, 30-50cm
Watsonville, Santa Cruz Co.	wat1	5	SILTY CLAY	0-10, 10-30, 30-50cm
Watsonville, Santa Cruz Co.	wat2	8	SANDY LOAM	0-10, 10-30, 30-50cm
Watsonville, Santa Cruz Co.	wat3	8	CLAY LOAM	0-10, 10-30, 30-50cm
Watsonville, Santa Cruz Co.	wat4	8	LOAM	0-10, 10-30, 30-50cm

General Soil Characteristics

In the comparison of soil properties below, Lost Hills 0-20cm, 20-40cm and 40-60cm soil data were lumped with the 0-10cm, 10-30 cm, and 30-50cm soil variability data, respectively (referred to as *layer 1*, *layer 2* and *layer 3*, respectively, below).

A. Pre-application WC- With the exception of 2 fields, layer 1 was much drier than layers 2 and 3, with layer 3 generally showing the highest water content (Figure 1).

B. Sat WC- Sat WC (=total porosity) was highest in the 0-10cm layer and decreased with depth (Figure 2).

C. Air-filled porosity - The combined net effect of *A.* and *B.* above is that the air-filled porosity at the time of sampling was greatest at the soil surface and decreased with depth (Figure 3). Air-filled porosity is calculated as (*Sat WC – WC*) and represents that portion of the soil matrix available for fumigant diffusive transport.

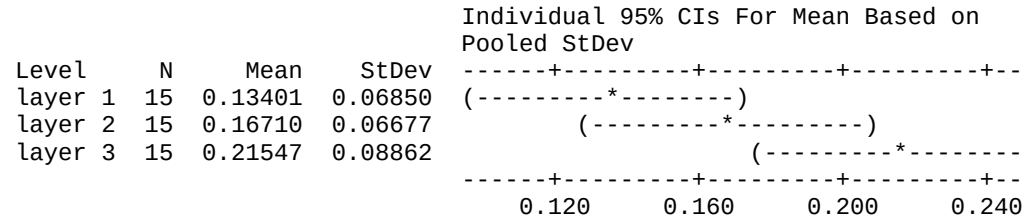

Figure 1. Field-mean pre-application soil-water content by soil layer

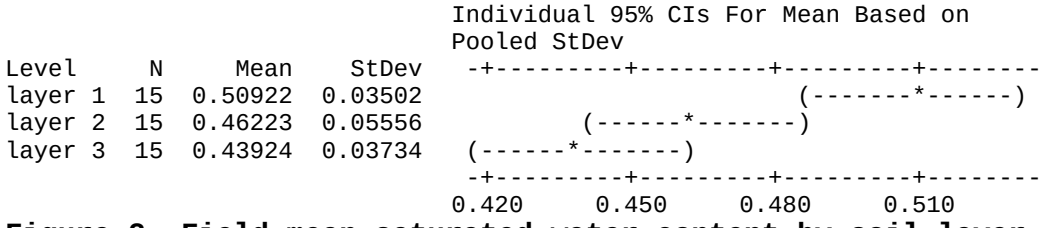

Figure 2. Field-mean saturated water content by soil layer

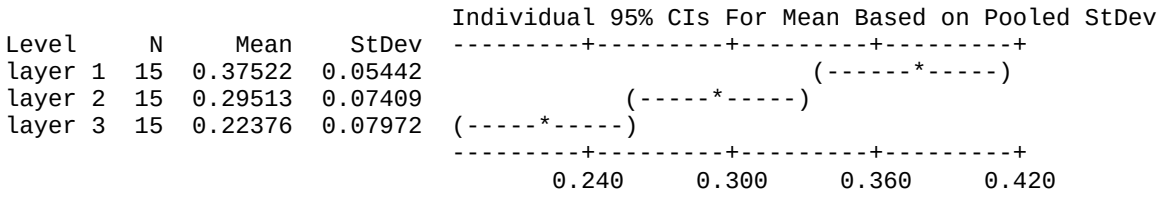

Figure 3. Field-mean air-filled porosity by soil layer

MODELING RESULTS

Comparison to field-based flux data

Field mean PIC and 13D ER and max flux for each field were calculated from the individual core simulation results (Figures 4 and 5; Table 2 - 5). In turn, the field results were used to calculate grand mean ER and max flux for each fumigant/application depth scenario. While the simulation results were highly variable within and between-fields, the grand ER means agree favorably with existing PIC and 13D ER estimates from field studies. Barry et al. (2007) report field-based ER estimates for shallow (12 inch) 13D and PIC untarped broadcast applications of 0.65 and 0.64, respectively, as compared to grand mean simulation estimates of 0.54 and 0.53 obtained here (Tables 2 -5). The field-based deep application (18 inch) 13D ER estimate is 0.26 (Barry et al., 2007), as compared to a simulated field-mean estimate of 0.34 here. No field-based deep application PIC flux data are given by Barry et al. (2007).

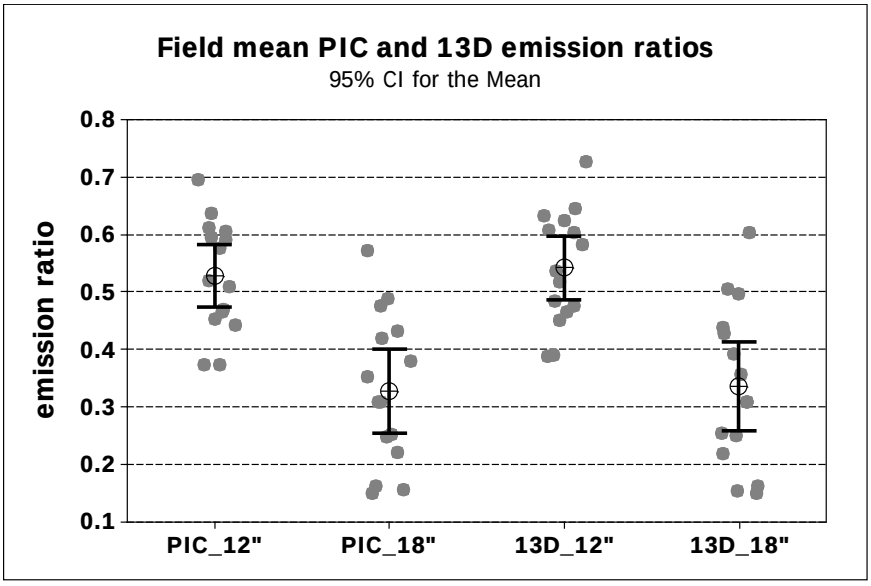

Figure 4. PIC and 13D field mean ER, *N*=15

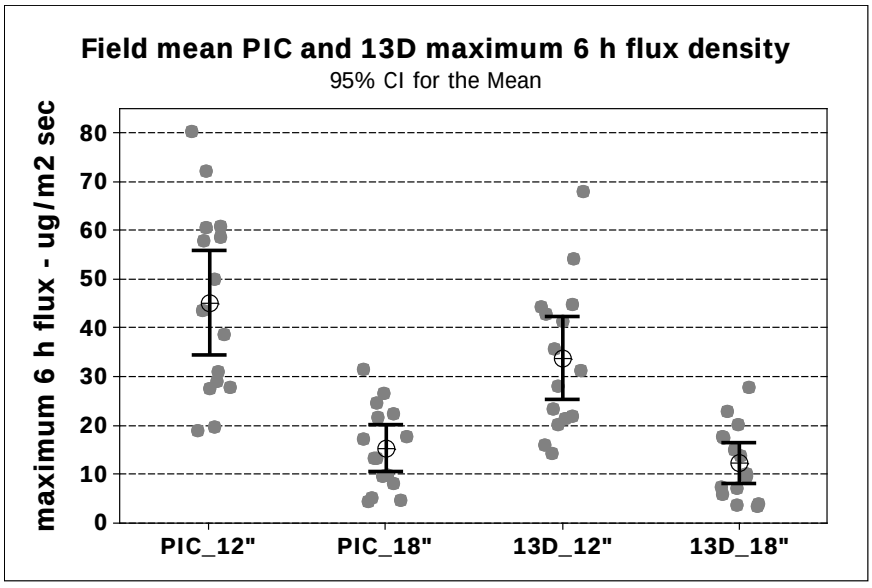

Figure 5. PIC and 13D field mean max flux, 100 lb/acre applied basis, *N*=15

Table 2. Field mean PIC emission ratios (ER) and maximum 6-hr flux density (Max flux, ug m^{-2} $sec^{-}1$, 100 lb $acre^{-1}$ applied basis). Number of simulations within each field = number of cores sampled, (Table 1). "Within CVs" are the within field coefficients of variation. Grand Mean is the mean of the 15 field means, the corresponding CV is the standard deviation of the 15 field means divided by the grand mean.

	12 Inch Application Depth				18 Inch Application Depth			
Field	**ER**	**ER CV (within)**	**Max flux**	**Max flux CV (within)**	**ER**	**ER CV (within)**	**Max flux**	**Max flux CV (within)**
cro1	0.636	0.101	72.2	0.296	0.433	0.155	22.4	0.229
din1	0.697	0.046	80.3	0.125	0.571	0.102	31.4	0.129
din2	0.612	0.096	57.8	0.325	0.477	0.155	24.7	0.269
LH1	0.453	0.167	27.7	0.369	0.253	0.341	9.9	0.557
LH2	0.373	0.062	19.0	0.102	0.149	0.149	4.4	0.195
LH3	0.374	0.272	19.8	0.390	0.163	0.322	5.2	0.385
mer1	0.510	0.148	38.7	0.438	0.309	0.232	13.3	0.406
san1	0.594	0.122	60.6	0.296	0.420	0.208	21.6	0.279
sto1	0.605	0.045	60.9	0.131	0.490	0.093	26.5	0.084
sto2	0.470	0.227	31.1	0.453	0.247	0.298	9.6	0.444
vis1	0.519	0.256	43.7	0.659	0.380	0.423	17.8	0.627
wat1	0.442	0.246	27.8	0.593	0.156	0.342	4.7	0.442
wat2	0.592	0.151	58.7	0.491	0.353	0.407	17.3	0.597
wat3	0.466	0.143	29.1	0.351	0.221	0.326	8.1	0.506
wat4	0.577	0.058	50.0	0.164	0.308	0.173	13.3	0.299

Table 3. Grand mean and between CV for PIC ER and max flux. Grand mean is the mean of the 15 field means; the between CV is the standard deviation of the 15 field means divided by the grand mean.

PIC Summary	12" ER	12" Max flux	18" ER	18" Max flux
grand mean	**0.528**	**45.2**	**0.329**	**15.4**
CV (between)	**0.184**	**0.429**	**0.401**	**0.559**
min	**0.373**	**19.0**	**0.149**	**4.4**
max	**0.697**	**80.3**	**0.571**	**31.4**

Table 4. Mean 13D emission ratios (ER) and maximum 6-hr flux density (Max flux, ug m^{-2} $sec^{-}1$, 100 lb $acre^{-1}$ applied basis). Number of simulations within each field = number of cores sampled, (Table 1). "Within CVs" are the within field coefficients of variation. Grand Mean is the mean of the 15 field means, the corresponding CV is the standard deviation of the 15 field means divided by the grand mean.

	12 Inch Application Depth				18 Inch Application Depth			
Field	**ER**	**ER CV (within)**	**Max flux**	**Max flux CV (within)**	**ER**	**ER CV (within)**	**Max flux**	**Max flux CV (within)**
cro1	0.645	0.097	54.2	0.304	0.439	0.155	17.8	0.263
din1	0.726	0.052	67.9	0.172	0.604	0.118	27.8	0.158
din2	0.634	0.093	44.3	0.404	0.496	0.157	20.2	0.286
LH1	0.465	0.155	21.3	0.278	0.255	0.343	7.5	0.525
LH2	0.390	0.056	14.2	0.152	0.149	0.150	3.5	0.174
LH3	0.389	0.252	15.9	0.390	0.164	0.313	4.0	0.341
mer1	0.518	0.142	28.0	0.308	0.309	0.232	10.0	0.430
san1	0.607	0.120	42.8	0.335	0.429	0.212	17.4	0.342
sto1	0.624	0.049	41.4	0.181	0.505	0.106	22.8	0.120
sto2	0.483	0.213	23.4	0.363	0.250	0.297	7.3	0.406
vis1	0.538	0.254	35.8	0.646	0.394	0.438	15.1	0.682
wat1	0.451	0.227	20.2	0.444	0.155	0.350	3.6	0.412
wat2	0.603	0.148	44.9	0.524	0.358	0.413	13.8	0.640
wat3	0.476	0.132	22.0	0.252	0.220	0.329	6.0	0.467
wat4	0.583	0.058	31.3	0.101	0.309	0.173	9.5	0.262

Table 5. Grand mean and between CV for 13D ER and max flux. Grand mean is the mean of the 15 field means; the between CV is the standard deviation of the 15 field means divided by the grand mean.

13D summary	**12" ER**	**12" Max flux**	**18" ER**	**18" Max flux**
grand mean	**0.542**	**33.8**	**0.336**	**12.4**
CV (between)	**0.183**	**0.453**	**0.418**	**0.610**
min	**0.389**	**14.2**	**0.149**	**3.5**
max	**0.726**	**67.9**	**0.604**	**27.8**

The differences in modeled flux among fields at a particular depth is due largely to differences in the soil moisture regime as it effects air-filled porosity (= *Sat WC – WC*). For example, Figure 6 illustrates the relationship between modeled maximum 6 hr PIC flux and air-filled porosity. Both *WC* and *Sat WC* are calculated using *BD*, so accurate measurement of this variable is important for simulating both cumulative and discrete flux.

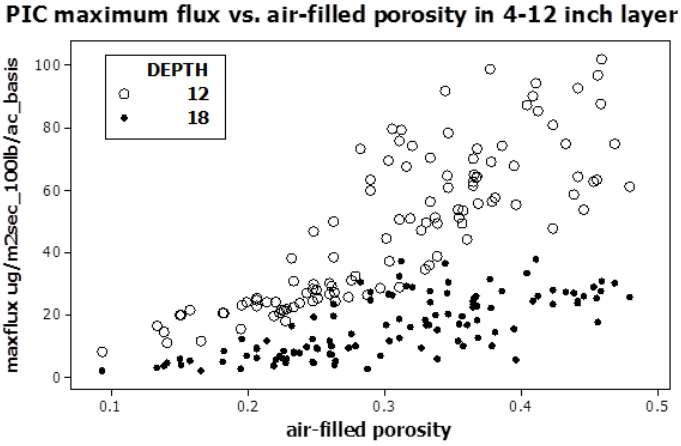

Figure 6. Modeled PIC maximum 6 hr flux vs air-filled soil porosity in layer 2 (4-12 inch depth). N=121 simulations for each depth.

For each of the 4 modeled fumigant-application depth combinations there was a strong correlation between-field mean max fluxes and ER (Figures 6 and 7). These linear relationships might be useful evaluating cumulative flux and discrete flux field data for consistency.

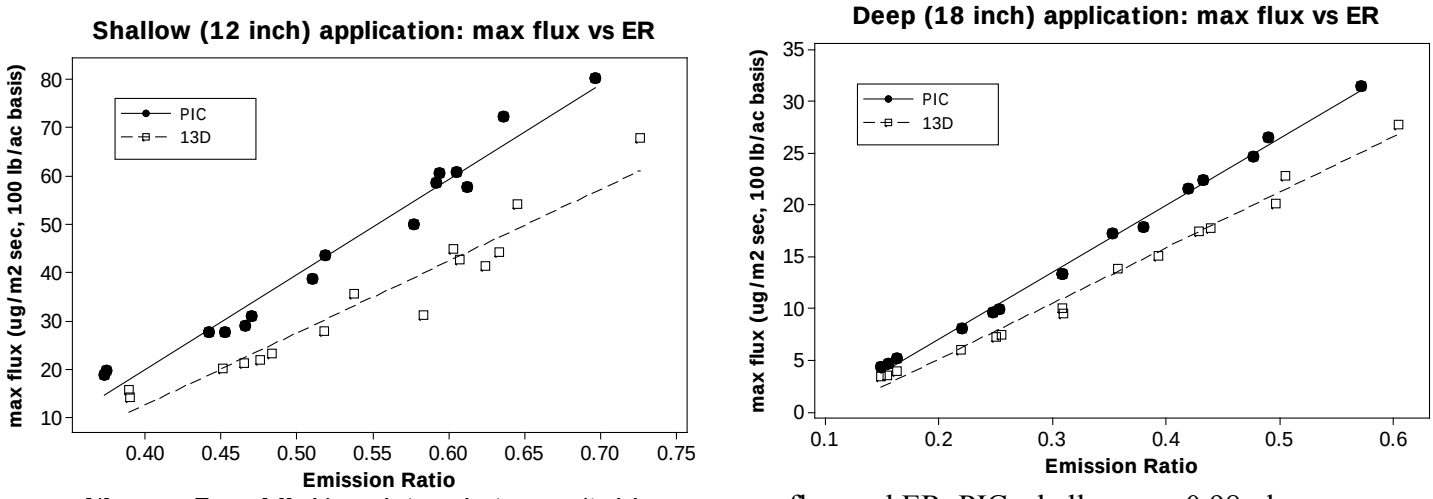

Figures 7 and 8. Correlation between-field mean max flux and ER. PIC: shallow, r = 0.98; deep, r=1.00. 13D: shallow, r = 0.96; deep, r=0.99.

Variability

ER and maxflux CVs were similar for PIC and 13D (Tables 2 - 5), and were greater for the deeper application depth as compared to the shallower depth. This is attributable to the greater influence on flux of variable soil properties at the deeper application depth. In nearly every case, max flux was more variable than ER regardless of application depth.

Plots of detail PIC and 13D ER and maximum fluxes by field visually suggest that the variability between-fields is greater than that within fields (Figure 9). An analysis of variance to quantify within versus between variance contributions is not formally possible because of different sampling designs among the fields. Soil cores were randomly sampled within each of the three Lost Hills fields while cores in the soil variability study were collected using a stratified random sampling scheme. In that sampling scheme, most fields had two soil cores collected in each of four field quadrants.

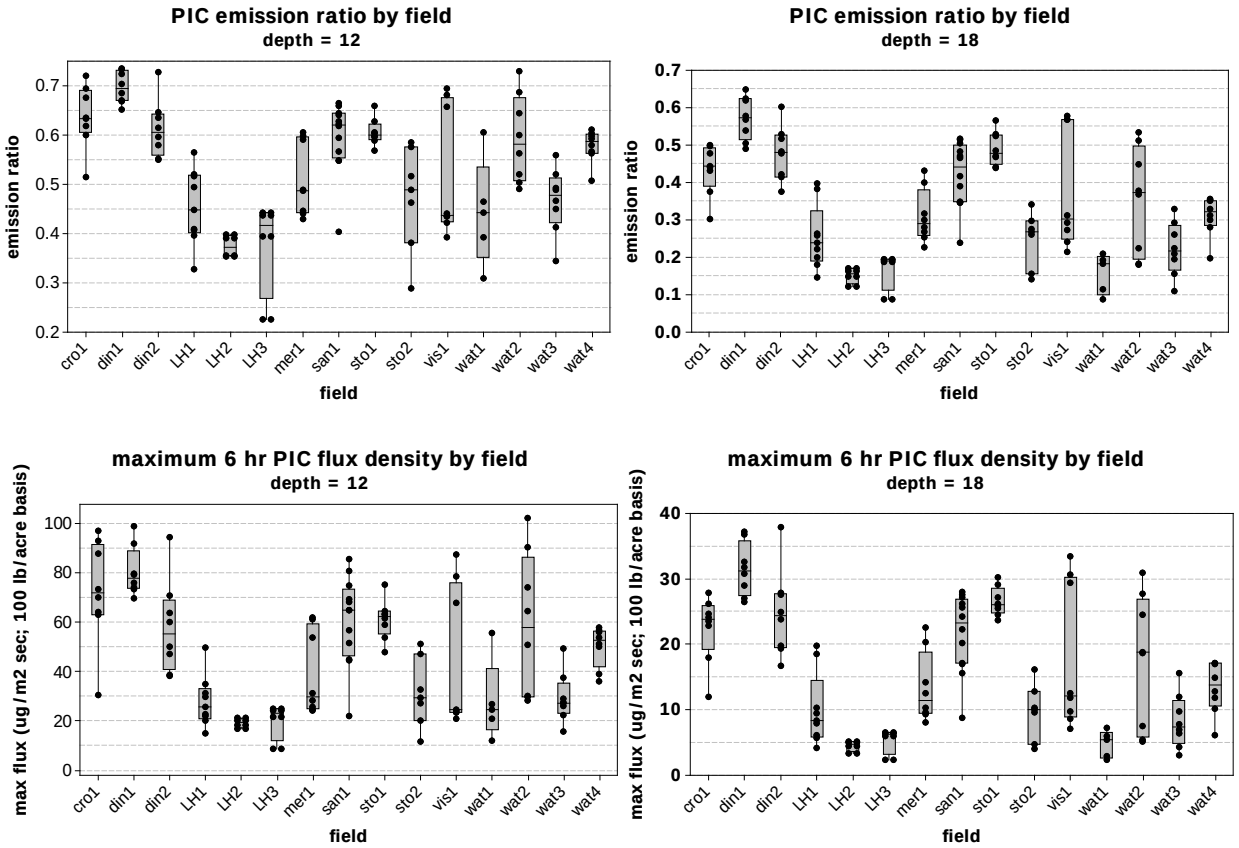

Figure 9. Detail PIC and 13D simulation data by field.

As an alternate approach, I compared between-field and within-field CVs for PIC and 13D ER and maxflux. This provides semi-quantitative comparisons of the relative magnitude of within vs between variability. For example, a cumulative frequency plot of the 18 inch PIC max flux within-field CVs is shown in Figure 10. The 15 within-field CVs were each calculated as the standard deviation of max flux within a field divided by the mean modeled max flux within that field. The vertical reference line overlay is located at the X axis value that is equivalent to the single between-field CV for that application scenario. The between-field CV is the standard deviation of the 15 field mean max fluxes divided by the grand mean of the max fluxes. Figure 10 shows that for the 18 inch deep PIC maximum 6 h flux case, the between CV corresponds to the 86th percentile of the within-field CV Normal distribution fit, and that within-field variability as measured by CV is lower than between-field variability in 13 of the 15 fields.

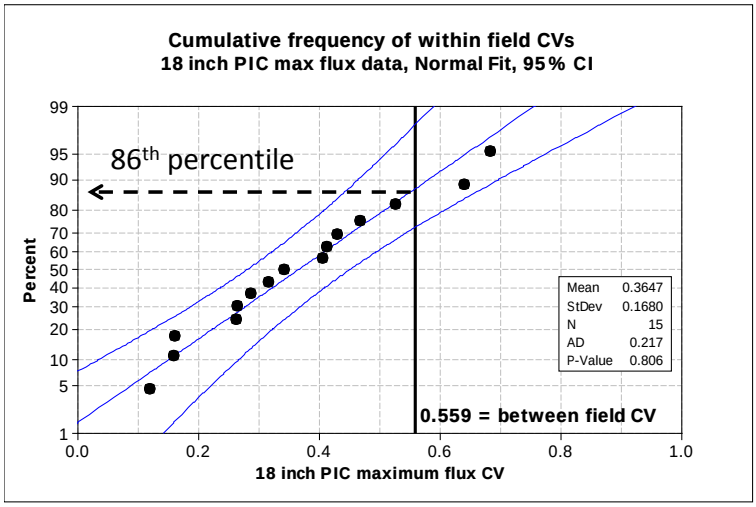

Figure 10. Comparison of within- and between-max flux CV for deep PIC application scenario

Table 6 summarizes the analysis of ER and max flux CVs for all application scenarios. The actual CV data are listed in Tables 2 and 3. In every scenario the within-field CVs were reasonably well described by a Normal distribution (A-D statistic, $p > 0.05$). The same analysis, conducted with standard deviations instead of CVs yielded essentially identical results: Between-field variability was generally greater than within-field variability for ER and max flux in the two application depths modeled, regardless of fumigant.

Table 6. Matching percentiles of within-field CVs for the observed between-field CVs

Fumigant	12 inch ER	12 inch max flux	18 inch ER	18 inch max flux
PIC	0.74	0.71	0.92	0.86
13D	0.75	0.87	0.94	0.91

Distribution of max flux data

One potential use of the field mean max flux data is for generating stochastic max flux estimates for use in Monte Carlo analyses of specific application scenarios. This typically entails fitting a distribution to the data and subsequent sampling of the fitted distribution. The 15 discrete field-mean max fluxes were adequately described by the Normal distribution based on a non-significant A-D test statistic (Figures 11, 12, $\alpha = 0.05$). However, several other distributions adequately fit the data based on the A-D statistic. These included log-Normal, Gamma and Weibull distributions. Therefore, a comprehensive distributional goodness-of-fit analysis should be conducted prior to Monte Carlo analysis.

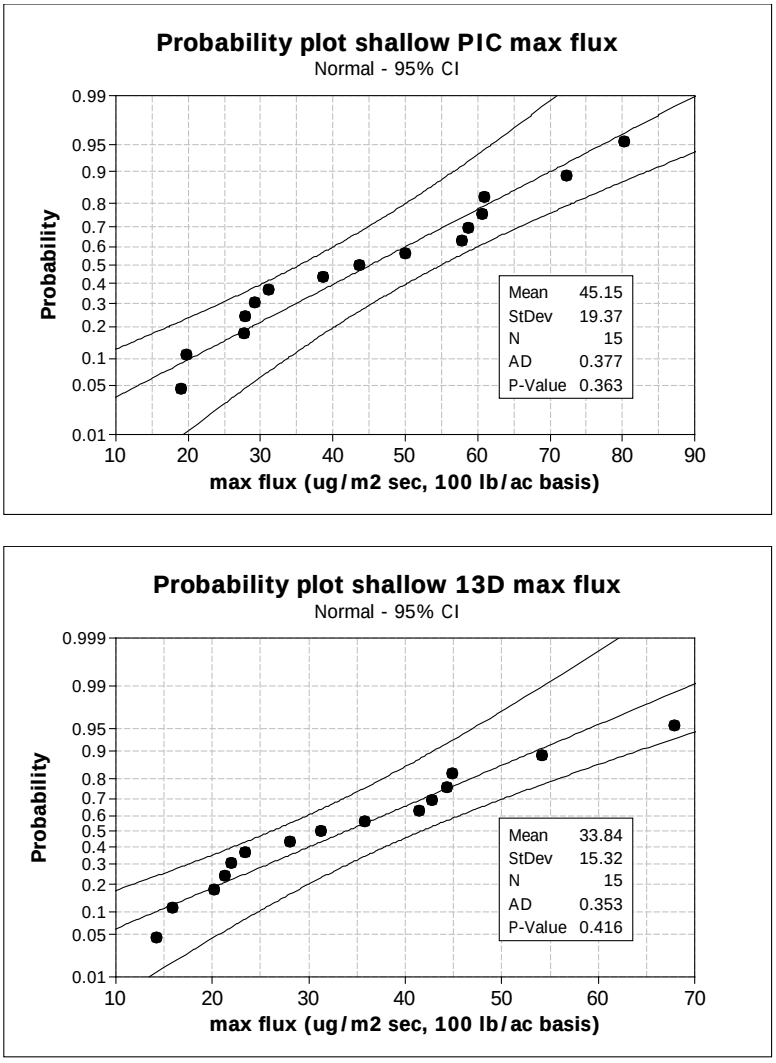

Figure 11. Normal distribution fits to PIC and 13D max flux data for shallow application scenario.

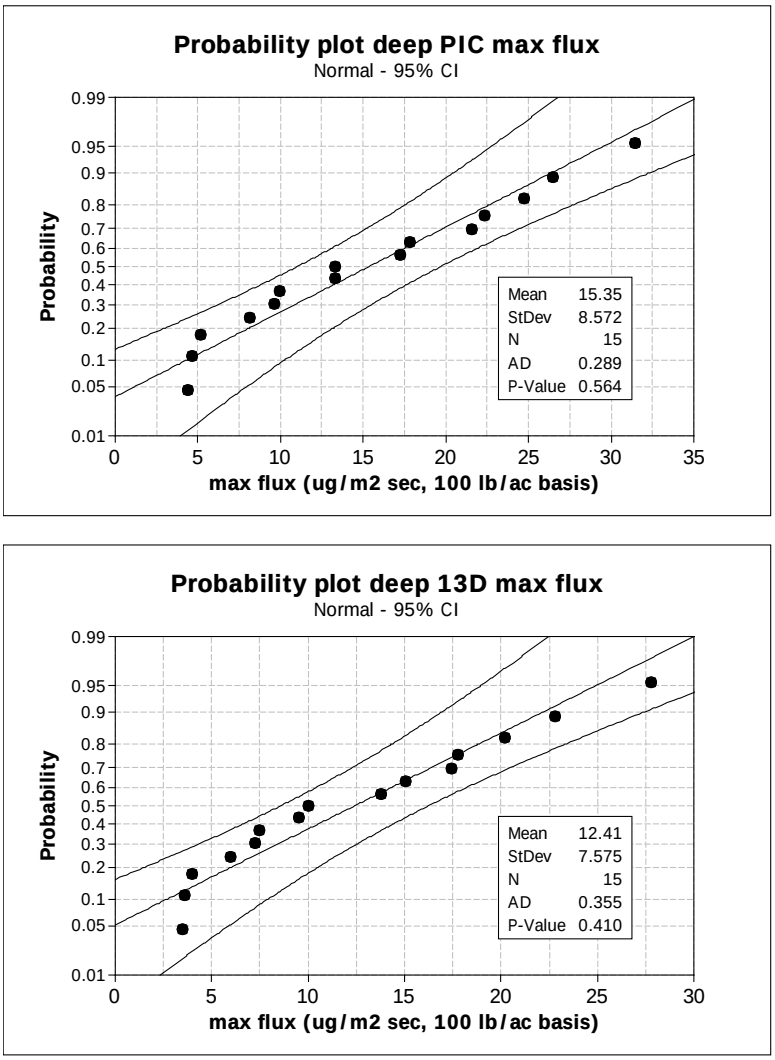

Figure 12. Normal distribution fits to PIC and 13D max flux data for deep application scenario.

REFERENCES

Barry, T., F. Spurlock and R. Segawa. September 29, 2007, memorandum to J. Sanders: Pesticide Volatile Organic Compound Emission Adjustments For Field Conditions And Estimated Volatile Organic Compound Reductions–Revised Estimates. On-line: http://www.cdpr.ca.gov/docs/emon/pubs/ehapreps/analysis_memos/1955_sanders.pdf

Freeze, R. A. and J. A. Cherry. 1979. Groundwater. Prentice-Hall, Inc. Englewood Cliffs, New Jersey

Johnson, B. and A. Tuli, 2013. Soil Sampling And Dynamic Monitoring of Temperature, Soil Moisture, Humidity, and Pressure During Bedded Fumigant Applications or Broadcast Fumigant Applications.

Spurlock, F., J. Šimùnek, B. Johnson and A. Tuli. 2013a. Sensitivity Analysis of Soil Fumigant Transport and Volatilization to the Atmosphere. Vadose Zone J. doi: 10.2136/vzj2012.0130.

Spurlock, F., B. Johnson, A. Tuli, S. Gao, J. Tao, F. Sartori, R. Qin, D. Sullivan, M. Stanghellini and H. Ajwa. 2013b. Simulation of Fumigant Transport and Volatilization from Tarped Broadcast Applications. Vadose Zone Journal. doi:10.2136/vzj2013.03.0056.

APPENDIX – MODELING DETAILS

Modeling domain: Simple rectangular geometry, 154 horizontal x 101 vertical nodal discretization

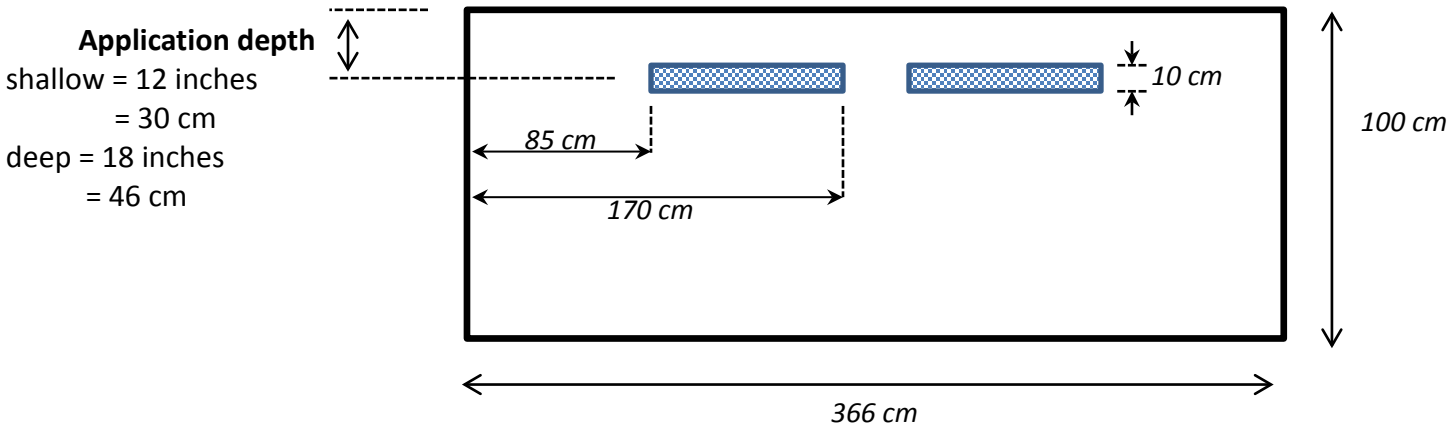

Boundary conditions:

Upper: water – atmospheric

solute – volatile

heat – first-type (Dirichlet) ; HYDRUS default sine wave;

$\overline{T} = 25C$, amplitude = 12C

Lower: water – free drainage

solute – third-type (Cauchy)

heat - third-type (Cauchy)

Initial conditions:

Water content: input data

Solute: see modeling domain above

Temperature: uniform profile 25C

Annotated example: Main HYDRUS Input File for PIC = Selector.in
The "# xxxxxx #" entries are soil core specific data input from measured data for simulations of each core.Initial water contents, solute concentration listed in input file DOMAIN.in. For additional information see HYDRUS documentation.

```
Pcp_File_Version=4
*** BLOCK A: BASIC INFORMATION ****************************************
Heading
Welcome to HYDRUS
LUnit  TUnit  MUnit  (indicated units are obligatory for all input data)
cm
days
ug
Kat (0:horizontal plane, 1:axisymmetric vertical flow, 2:vertical plane)
  2
MaxIt   TolTh   TolH InitH/W  (max. number of iterations and tolerances)
  10    0.001      1     t
lWat lChem lSink Short Inter lScrn AtmIn lTemp lWTDep lEquil lExtGen lInv
 t     t     f     t     f    t     t     t     f      t      f      f
lUnsatCh lCFSTr   lHP2   m_lActRSU lDummy  lDummy  lDummy
 f       f       f       f       f       f       f
 PrintStep  PrintInterval lEnter
         1              0       f
*** BLOCK B: MATERIAL INFORMATION ***************************************
NMat    NLay    hTab1   hTabN     NAniz
  4       1    0.0001   10000
    Model   Hysteresis
      0          0
  thr    ths          Alfa      n          Ks      l
 0.0 #   thetaS1   #  0.036   1.56      24.96    0.5
 0.0 #   thetaS2   #  0.036   1.56      24.96    0.5
 0.0 #   thetaS3   #  0.036   1.56      24.96    0.5
 0.0 #   thetaS4   #  0.036   1.56      24.96    0.5
*** BLOCK C: TIME INFORMATION ****************************************
        dt       dtMin       dtMax     DMul    DMul2  ItMin ItMax  MPL
     0.0001      1e-005       0.005     1.3     0.7     3     7    48
      tInit        tMax
       0.25       12.25
TPrint(1),TPrint(2),...,TPrint(MPL)
        0.5        0.75           1        1.25         1.5        1.75
          2        2.25         2.5        2.75           3        3.25
```

Soil hydraulic properties: 4 soil layers, Lost Hills layer 4 = 60-80 cm measured data, remaining fields layer 4 properties = layer 3. All theta residual, thetaS"x"= saturated water content layer "x"; alpha, n, Ks, l = default loam properties

initial time= application time = 0.25 days. Tmax = simulation end = 12.25 days

```
        3.5        3.75           4        4.25         4.5        4.75
          5        5.25         5.5        5.75           6        6.25
        6.5        6.75           7        7.25         7.5        7.75
          8        8.25         8.5        8.75           9        9.25
        9.5        9.75          10       10.25        10.5       10.75
         11       11.25        11.5       11.75          12       12.25
*** BLOCK D: SOLUTE TRANSPORT INFORMATION **********************************************
 Epsi  lUpW  lArtD lTDep  cTolA  cTolR   MaxItC  PeCr  Nu.ofSolutes Tortuosity Bacter Filtration
  0.5     f     f     t       0    0     1       2        1          t         f         f
lWatDep    lInitM  lInitEq  lTortM  lFumigant lDummy  lDummy lDummy  lDummy  lDummy lDummy
  f         t        f        t        t         f       f      f       f       f      f
Bulk.d.     DisperL.      DisperT     Frac      ThImob (1..NMat)
#  BD1      #          15           3           1           0
#  BD2      #          15           3           1           0
#  BD3      #          15           3           1           0
#  BD4      #          15           3           1           0
DifW       DifG               n-th solute
0.707        6515
Ks       Nu  Beta  Henry    SnkL1    SnkS1    SnkG1  SnkL1' SnkS1' SnkG1' SnkL0 SnkS0 SnkG0 Alfa
0.134     0    1   0.083   0.15553  0.15553  0.15553   0      0      0      0     0     0    0
0.106     0    1   0.083   0.15553  0.15553  0.15553   0      0      0      0     0     0    0
0.052     0    1   0.083   0.15553  0.15553  0.15553   0      0      0      0     0     0    0
0.0       0    1   0.083   0.15553  0.15553  0.15553   0      0      0      0     0     0    0
Temperature Dependence
 DifW       DifG               n-th solute
 17920       4566
  Ks    Nu   Beta  Henry SnkL1 SnkS1 SnkG1  SnkL1' SnkS1' SnkG1' SnkL0  SnkS0  SnkG0   Alfa
  0     0     0    39120 56933 56933 56933     0     0      0     0      0       0      0
 cTop    cBot
  0        0         0     0     0     0       0     0    0.5
  tPulse
     10
  AddFumigant
         f
*** BLOCK E: HEAT TRANSPORT INFORMATION *************************************************
    Qn           Qo  Disper.  B1       B2          B3          Cn          Co          Cw
#    solids1  #   0    5       1 1.56728e+016 2.53474e+016 9.89388e+016 1.43327e+014 1.8737e+014 3.12035e+014
#    solids2  #   0    5       1 1.56728e+016 2.53474e+016 9.89388e+016 1.43327e+014 1.8737e+014 3.12035e+014
#    solids3  #   0    5       1 1.56728e+016 2.53474e+016 9.89388e+016 1.43327e+014 1.8737e+014 3.12035e+014
#    solids4  #   0    5       1 1.56728e+016 2.53474e+016 9.89388e+016 1.43327e+014 1.8737e+014 3.12035e+014
       TTop        TBot
          0           0          0          0          0          0
      tAmpl     tPeriod
         12           1
```

Tortuosity = Moldrup model

BD "x" = bulk density layer "x". Ks= linear distribution coefficient calculated from Lost Hills calibrated PIC KOC and OC contents layer 1-4 of of 0.37, 0.30, 0.14, and 0.00.

Bulk degradation rate constant = 0.15553 day-1= calibrated in Lost Hills for PIC

Solids "x" = volume fraction solids in layer "x". Calculated as 1-thetaS"x". Heat transport parameters = default for Loam soils

*** END OF INPUT FILE 'SELECTOR.IN' **********

Table A-1. Principal input variables required for HYDRUS simulations.

Input Variable (units)	Variable name	Source
ρ_b (cm^3(gm soil)$^{-1}$)	soil bulk density[A]	Measured each core
θ_s (-)	saturated water content[A]	calculated from bulk density (θ_s = 1- ρ_b/2.65)
θ_i (-)	initial water content[A]	Measured each core
θ_r (-)	residual water content[A]	Assumed = 0
α (cm^{-1})	VG retention model parameter[A, B]	loam texture class mean (Carsel and Parrish, 1988)
n (-)	VG retention model parameter[A, B]	loam texture class mean (Carsel and Parrish, 1988)
K_s (cm d^{-1})	saturated hydraulic conductivity[A]	loam texture class mean (Carsel and Parrish, 1988)
C_n (J cm^3 K^{-1})	volumetric solid phase heat capacity[A]	HYDRUS Loam default
λ_L, b_1, b_2, b_3	soil thermal conductivity parameters[A]	Horton and Chung (1991)
$T_0(t)$ (C)	soil surface temperature as function of time *t*	HYDRUS sine wave, mean T=25C, amplitude = 12C
D_g (cm^2 d^{-1})	gas phase diffusion coefficient	SPARC on-line calculator (Hilal et al., 2003a, 2003b)
D_gE_a (J mol^{-1})	D_g activation energy[C]	SPARC on-line calculator (Hilal et al., 2003a, 2003b)
D_w (cm^2 d^{-1})	aqueous phase diffusion coefficient	SPARC on-line calculator (Hilal et al., 2003a, 2003b)
D_wE_a (J mol^{-1})	D_w activation energy[C]	SPARC on-line calculator (Hilal et al., 2003a, 2003b)
K_h (-)	Henry's law constant	*chloropicrin:* Kawamoto and Urano (1989); *1,3-D*: Wright, (1992)
K_hE_a (J mol^{-1})	K_h activation energy[C]	*chloropicrin:* Chikos and Acree (2006); *1,3-D*: Wright, (1992)
k_1 (d^{-1})	first-order degradation rate constant[A]	Calibrated profile mean dgrd rate (Spurlock et al., 2013)
k_1E_a (J mol^{-1})	k_1 activation energy[A,C]	mean [data of Dungan et al. (2003) and Gan et al. (2000)]
OC (g OC (g $soil^{-1}$)	soil organic carbon mass fraction[A]	Lost Hills mean of 3 fields
K_d (ml^3 g^{-1})	soil partition coefficient[A]	calculated from **calibrated** K_{OC} and measured OC (K_d = K_{OC} * OC) (Spurlock et al., 2013)
d (cm)	tarp boundary layer depth[D]	bare ground default (Jury et al., 1986)
λ_w (cm)	longitudinal dispersivity	HYDRUS default

[A] required for each soil layer

[B] van Genuchten (VG) soil-water retention model was used (van Genuchten, 1980)

[C] activation energies describe the temperature dependence of the associated parameter (Spurlock et al., 2013)

[D] tarp boundary layer depth (describes tarp permeability).

Table A-2. Chemical Property data used for HYDRUS simulations.

Input Variable (units)	**Variable name**	**Source**
D_g (cm^2 d^{-1})	gas diffusion coefficient *chloropicrin:* 6515 *13D:* 6886	SPARC on-line calculator (Hilal et al., 2003a, 2003b)
D_gE_a (J mol^{-1})	D_g activation energy *chloropicrin:* 4566 *13D:* 4560	SPARC on-line calculator (Hilal et al., 2003a, 2003b)
D_w (cm^2 d^{-1})	aq. diffusion coefficient *chloropicrin:* 0.707 *13D:* 0.735	SPARC on-line calculator (Hilal et al., 2003a, 2003b)
D_wE_a (J mol^{-1})	D_w activation energy *chloropicrin:* 17920 *13D:* 18035	SPARC on-line calculator (Hilal et al., 2003a, 2003b)
K_h (-)	Henry's constant. *chloropicrin:* 0.083 *13D:* 0.050	*chloropicrin:* Kawamoto and Urano (1989); *1,3-D*: Wright, (1992)
K_hE_a (J mol^{-1})	K_h activation energy *chloropicrin:* 39120 *13D:* 32085	*chloropicrin:* Chikos and Acree (2006); *1,3-D*: Wright, (1992)
k_1 (d^{-1})	degradation constant *chloropicrin:* 0.1555 *13D:* 0.0968	calibrated in Lost Hills field 1, Spurlock et al., 2013
k_1E_a (J mol^{-1})	k_1 activation energy *chloropicrin:* 56933 *13D:* 59028	mean [data of Dungan et al. (2003) and Gan et al. (2000)]
K_{OC} ml (g OC)$^{-1}$	OC-normalized soil partition coefficient. *chloropicrin:* 66 *13D:* 28	calibrated in Lost Hills field 1, Spurlock et al., 2013
d (cm)	boundary layer depth (tarp permeability) *chloropicrin:* 0.5 cm *13D:* 0.5 cm	bare ground value (Jury et al., 1986

Appendix References

Carsel, R.F. and R.S. Parrish. 1988. Developing Joint Probability Distributions of Soil Water Retention Characteristics. Water Resources Research 24:755-769.

Chickos, J.S. and W.E. Acree, Jr. 2003. Enthalpies of Vaporization of Organic and Organometallic Compounds, 1880–2002. J. Phys. Chem. Ref. Data, Vol. 32: 519-878.

Dungan, R.S. and S.R. Yates. 2003. Degradation of Fumigant Pesticides: 1,3-Dichloropropene, Methyl Isothiocyanate, Chloropicrin, and Methyl Bromide. Vadose Zone J. 2:279-286.

Gan, J., S.R. Yates, F.F. Ernst, and W.A. Jury. 2000a. Degradation and Volatilization of the Fumigant Chloropicrin after Soil Treatment. Environ. Qual. 29:1391–1397.

Hilal, S.H., S.W. Karickhoff and L.A. Carreira. 2003a. Prediction of Chemical Reactivity Parameters and Physical Properties of Organic Compounds from Molecular Structure using SPARC. USEPA publication 600/R-03/030. Available at: <http://www.epa.gov/athens/publications/reports/EPA_600_R03_030.pdf>.

Hilal, S.H., S.W. Karickhoff and L.A. Carreira. 2003b. Verification and Validation of the SPARC Model. USEPA publication 600/R-03/033. Available at: <http://www.epa.gov/athens/publications/reports/EPA_600_R03_033.pdf>.

Horton, R. and S. Chung. 1991. Soil Heat Flow. In: J. Hanks and J.T. Ritchie (Editors), Modeling Plant and Soil Systems. American Society of Agronomy, Inc., Madison, WI, pp. 397-438.

Jury, W.A., W.F. Spencer and W.J. Farmer. 1986. Behavior Assessment Model for Trace Organics in Soil: I. Model Description. J. Env. Qual 12:558-564.

Spurlock, F., B. Johnson, A. Tuli, S. Gao, J. Tao, F. Sartori, R. Qin, D. Sullivan, M. Stanghellini and H. Ajwa. 2013. Simulation of Fumigant Transport and Volatilization from Tarped Broadcast Applications. Vadose Zone Journal. doi:10.2136/vzj2013.03.0056.

Kawamoto,K., and K. Urano. 1989. Parameters for predicting fate of organochlorine pesticides in the environment (I) Octanol-water and air-water partition coefficients. Chemosphere 18:1987-1996.

Wright, D.A., Sandler, S.I. and D. DeVoll. 1992. Infinite dilution activity coefficients and solubilities of halogenated hydrocarbons in water at ambient temperatures. Environ. Sci. Technol. 26:1928-1931.